J. Physiol. (1982), **324**, *pp.* 297–318
With 12 text-figures
Printed in Great Britain

ACTIVATION AND INACTIVATION CHARACTERISTICS OF THE SODIUM PERMEABILITY IN MUSCLE FIBRES FROM *RANA TEMPORARIA*

BY CAROL A. COLLINS*, E. ROJAS AND B. A. SUAREZ-ISLA†
From the Department of Biophysics, School of Biological Sciences, University of East Anglia, Norwich NR4 7TJ

(*Received 6 March 1981*)

SUMMARY

1. The steady-state and kinetic characteristics of the processes of activation and inactivation of the Na^+ permeability, P_{Na}, were measured in cut skeletal muscle fibres from *Rana temporaria* under voltage-clamp conditions.

2. The specific resistance, r_{ss}, in series with the surface sarcolemma, was estimated as 6 Ω cm^2 by measuring the initial value of the membrane potential transient in response to current pulses under current-clamp conditions. To reduce the error in the potential across the sarcolemma introduced by r_{ss}, Na^+ currents were recorded using positive feed-back compensation, in the presence of tetrodotoxin (2·4–5 nM).

3. $P_{Na}(t)$ was fitted with m^3h kinetics assuming a voltage-dependent delay, δt, to the start of the activation process.

4. The P_{Na}–V_p curve exhibited saturation at potentials more positive than 30 mV. m_∞, calculated as $(P_{Na,\infty}/\bar{P}_{Na})^{\frac{1}{3}}$ as a function of V_p, was a sigmoid curve with a mid point at −35 mV. The slope, dm_∞/dV_p, at this point was 0·032 mV^{-1}.

5. Using a double-pulse protocol a non-exponential time course for the development of fast inactivation at small depolarizations was observed.

6. The time constant for activation, τ_m, as a function of V_p, and τ_h as a function of V_p, could be fitted with an approximately bell-shaped function, maximum of 430 μs at −43 mV and 925 μs at −78 mV respectively, at 15 °C.

7. The mid-point potential of the h_∞–V_1 curve occurred at −58 mV, and h_∞ approached 1 for V_1 values more negative than −103 mV.

8. Using a double-pulse procedure the development of a slow inactivation of the Na^+ current was demonstrated. Its time course could be described in terms of a single exponential function, time constant equal to 0·58 s. The recovery from slow inactivation could be described by a similar exponential for recovery times smaller than 1 s.

INTRODUCTION

On the basis of their kinetic model, Hodgkin & Huxley (1952*b*) predicted that a fraction of the current flowing across an excitable membrane when ionic channels are

* Formerly Carol A. Harvey.
† Present address: Laboratory of Neurosciences, Gerontology Research Center, Baltimore City Hospitals, Baltimore, MD 21224, U.S.A.

TABLE 1. Composition of solutions for muscle fibre

Solution*	Osmotic pressure (mosmol)	Na^+	K^+	Cs^+	Ca^{2+}	Mg^{2+}	Tris	TEA^+	Cl^-	F^-	Is^-	SO_4^{2-}	EGTA	TTX
		(mM)												(nM)
A 1 (K^+-free Ringer, chloride)	225	118	—	—	1·8	—	5	10	136·6	—	—	—	—	—
A 2 (K^+-free Ringer, chloride, TTX)	245	118	—	—	1·8	—	5	20	146·6	—	—	—	—	5 or 2·4
A 3 (K^+-free Ringer, sulphate, TTX)	220	140	—	—	1·8	—	5	20	28·6	—	—	70	—	5
A 4 (Na^+- and K^+-free Ringer, Tris chloride, TTX)	227	—	—	—	1·8	—	123	20	146·6	—	—	—	—	230
A 5 (Na^+- and K^+-free Ringer, Tris sulphate, TTX)	167	—	—	—	1·8	—	140	20	3·6	—	—	90	—	230
B (NaIs solution)	227	100	—	—	—	10	1	—	21·0	—	100	—	—	—
E and C (CsF solution)	250	4	2·2	118	—	—	1	20	2·0	118	20	—	1·1	—
High-Mg^{2+}/low-Ca^{2+} Ringer	220	116	2·5	—	0·5	10	5	—	144·5	—	—	—	—	—

Ca^{2+} activities and electrical conductivities were compared between sulphate and chloride solutions.
Ca^{2+} activity ratio, $[Ca^{2+}]_{A3}/[Ca^{2+}]_{A2}$ was measured as 0·3 using a Ca^{2+} electrode.
Electrical conductivity ratio, for A 2/A 3 = 1·11, for A 4/A 5 = 1.21.
* A, B, C and E refer to pools in experimental chamber.

activated would be due to movement of charges associated with channel gating. Recently, a non-linear component of the fast capacitative current has been detected in skeletal muscle fibres (Vergara & Cahalan, 1978) which presumably holds a functional relation to the gating of the Na^+ channel in these fibres. In order to study the relationships involved, the kinetic and steady-state properties of the Na^+ current and the non-linear capacity must be studied in parallel, that is on the same preparation and using the same methods. In this and the following paper a vaseline-gap voltage-clamp system with potentiometric recording was applied to cut single muscle fibres to produce comparable data for this purpose.

This paper deals with the activation and inactivation characteristics of the Na^+ permeability, as defined by the m^3h system (Hodgkin & Huxley, 1952*b*), while the second paper (Collins, Rojas & Suarez-Isla, 1982) describes the measurement of fast charge movement in these fibres, and explores the possibility of identifying the non-linear component with the movement of the m gating particles.

METHODS

Single muscle fibres (segments 10–15 mm in length) were dissected in high Mg^{2+}/low Ca^{2+} Ringer solution (composition of solutions given in Table 1) from the extensor cruris muscle of *Rana temporaria*, and mounted in a Plexiglass chamber originally designed for work with myelinated nerve fibres (Nonner, 1969). The essential features are four pools formed by two movable troughs and a middle partition (80 μm width). The width of the voltage-measuring pool (A) and ground pool (B) could thus be adjusted (40–100 μm and 80–100 μm respectively) giving an approximate volume of 100 μl for each. The volumes of the non-adjustable pools (electrically connected to the input (C) and output (E) of the feed-back amplifier) were 250 and 100 μl. The small internal trough used to form the air gap between the input pool and ground (Nonner, 1969) was removed. Vaseline cylinders (80 μm diameter) were placed against the internal borders of the pools E and C to increase the length of the hydrophobic pathway.

Before mounting the fibre the chamber was coated with a thin layer of silicone grease. The fibre was then transferred to the chamber under the sodium isethionate (NaIs) solution used in the ground pool. A second set of vaseline seals were placed along the partitions to hold the fibre horizontally and to isolate the four pools. The ends of the fibre were cut in CsF solution containing the Ca^{2+}-chelating agent EGTA (ethyleneglycol-bis-(β-aminoethylether) *N,N'*-tetraacetic acid), and the voltage-measuring pool was continuously perfused with a K^+-free Ringer solution.

Two voltage-clamp systems were used in these experiments, the single control amplifier voltage clamp (Nonner, 1969) and the double control amplifier configuration (Dodge & Frankenhaeuser, 1958) with modifications by Hille & Campbell, 1976. Voltage-clamp circuitry for the latter system, as used here, has been described in detail (Quinta-Ferreira, Arispe & Rojas, 1982). The high speed data acquisition system (Pynsent & Rojas, 1979) was common to both clamps.

The resting potential of the fibre in pool A was measured with micro-electrodes (50×10^6 Ω tip resistance), taking the potential of the solution in the ground pool as reference. With the four extracellular electrodes in position and minimum amplifier gain, the measured membrane potential was less than 1 mV (eight measurements in two fibres) and unaffected by removal of the current-injecting electrode in pool E. The potential difference between the A and B pools followed the commanded voltage levels to within 1 %.

Membrane current was calculated from the measured voltage using the resistance of the proximal end of the fibre, R_{ED} (D is a point within the myoplasm in pool A) calculated by two methods: as $10^3 \times V_E/V^*$, where V_E represents the voltage at electrode E, and V^* is the voltage drop across a 10^3 Ω resistance in series with this electrode; as $\rho l/\pi r^2$, where l is the distance from the cut end of the fibre in pool E to the edge of the vaseline seal facing pool A, r is the radius of the fibre and ρ is the specific resistivity of the myoplasm (average measurement, 111 Ω cm). A comparison of the average value for R_{ED} obtained by the two methods gave 86×10^3 Ω and 87×10^3 Ω (two fibres) respectively, indicating a difference of less than 2 %.

The non-rectifying component of the leakage current was compensated electronically, and positive feed-back compensation for the effects of the resistance in series with the sarcolemma was used in experiments performed with the clamp in the Dodge–Frankenhaeuser configuration. In addition, all fibres were treated externally with tetrodotoxin (TTX) at a concentration close to the dissociation constant in these fibres (2·4–5 nM; Allen, Rojas & Suarez-Isla, 1980). The difference in time course of the Na^+ currents with 0 nM- and 4 nM-TTX is shown for one fibre in which the effects of a large uncompensated series resistance were particularly noticeable (Fig. 1).

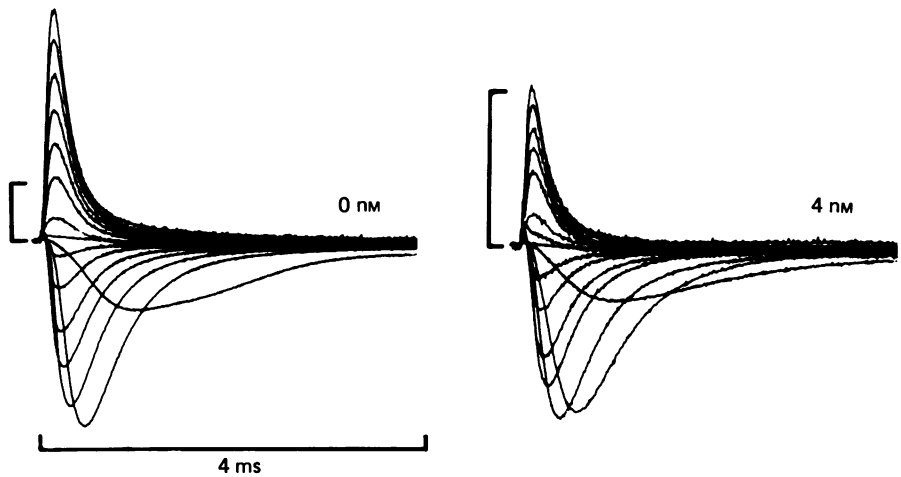

Fig. 1. Effect of series resistance on time course. Pool A perfused with K^+-free Ringer solution containing TTX (concentration of TTX given in nM above each record), at 18 °C. Fibre treated internally with E and C solution. Holding potential set at −90 mV. Series of Na^+ currents for absolute value of the membrane potential increasing in 10 mV steps from −40 to 100 mV. Area of membrane in pool A is $2·9 \times 10^{-4}$ cm². Vertical bars indicate 1·0 μA.

RESULTS

Measurement of series resistance

The voltage drop across the resistance in series with the surface sarcolemma, R_{ss}, was measured as V_0/i_0, where V_0 is the size of the initial jump in the voltage transient in response to a current pulse, i_0, under current-clamp conditions (Moore & Cole, 1963; Keynes, Rojas, Taylor & Vergara, 1973) as illustrated in Fig. 2*A*. The average value

Fig. 2. *A*, measurement of series resistance. Pool A perfused with solution A1 at 17·5 °C. Cut ends in solution E and C. Membrane potential estimated as −90 mV. Photographic recording of membrane potential transients under current-clamp conditions. For upper traces depolarizing current pulse produced a voltage deflexion $V_E = 20$ mV; for lower traces hyperpolarizing current pulse, $V_E = -20$ mV. i_0 is calculated as V_E/R_{ED}, where R_{ED} was determined from geometrical measurements of the fibre as 69 kΩ. R_{ss} estimated as V_0/i_0, 8·6 kΩ. Area of membrane in pool A, $3·14 \times 10^{-4}$ cm². The specific series resistance, r_{ss}, calculated with this area, 2·7 Ω cm².Using the correction factor 1·89 (see Collins *et al.* 1982), $r_{ss} = 5·1$ Ω cm². *B*, muscle action potential. Photographic recording of action potential under current-clamp conditions in response to current pulses that took the membrane potential to −65 mV.

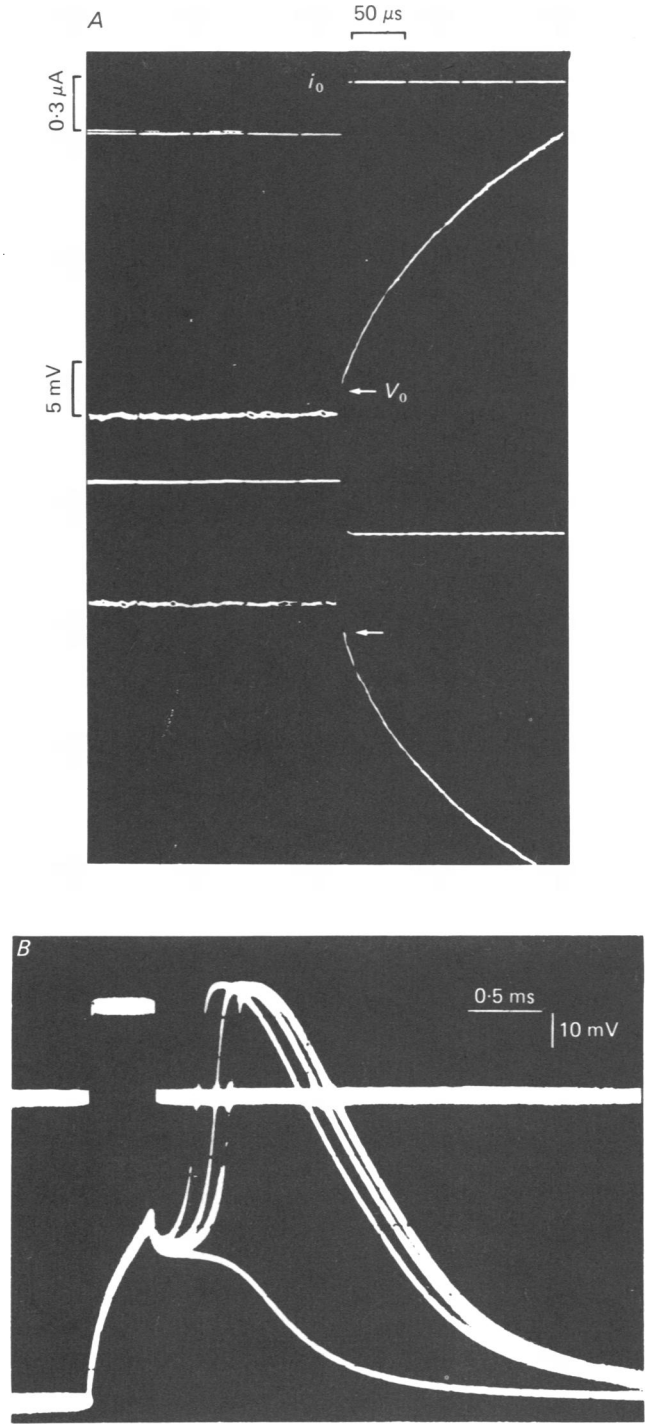

Fig. 2. For legend see opposite.

for R_{ss} was $8 \times 10^3\ \Omega$ for an average surface membrane area of 4×10^{-4} cm^2. In the following paper it is proposed that the electrically effective surface membrane is 1·89 times larger than the area calculated as πdl (d = diameter of the fibre in pool A, l = distance between the vaseline seals on either side of pool A), whence the specific series resistance is calculated as $8 \times 10^3\ \Omega \times 4 \times 10^{-4}$ cm^2 $\times$ 1·89 = 6 Ω cm^2.

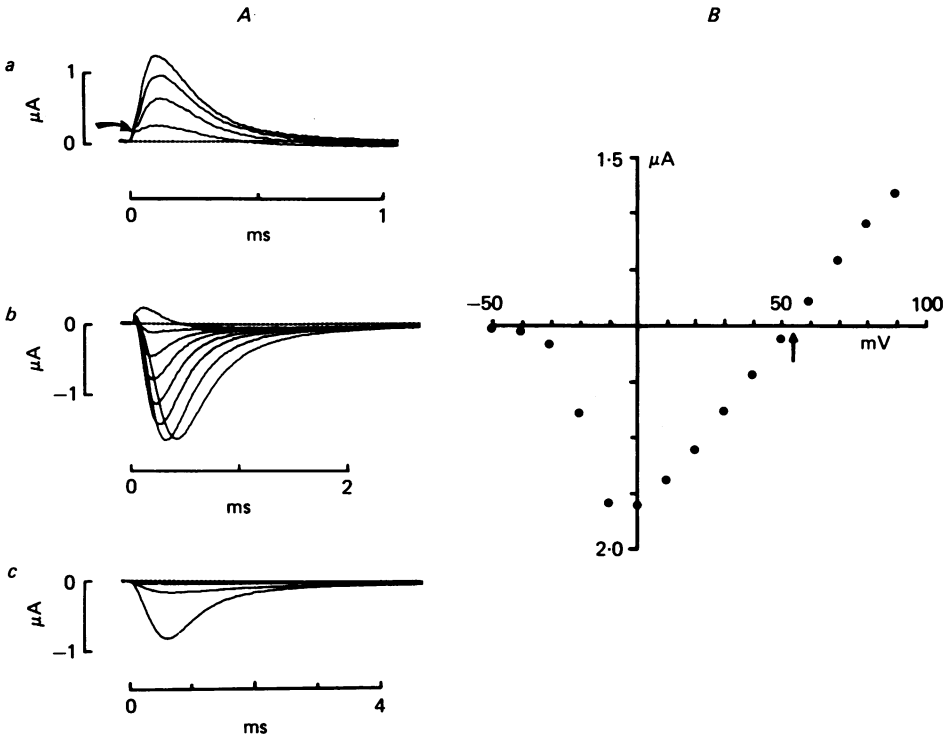

Fig. 3. Na^+ currents and current–voltage relation. Pool A perfused with solution A 1 at 17 °C. Cut ends in solution E and C. Holding potential = −100 mV. Surface membrane area in pool A = $2{\cdot}60 \times 10^{-4}$ cm^2. *A*, each record represents the sum of the current transients in response to a depolarizing test pulse, with the current transient in response to a 50 mV control hyperpolarizing pulse scaled by the ratio of test/control pulse. Time base magnified according to settling level for the current. Dashed lines indicate zero. Absolute value of the membrane potential during the pulse, V_p, in the ranges: bottom, −50 to −20 mV; middle, −10 to 60 mV; top, 60 to 90 mV. Arrow indicates position of initial outward transient attributed to charge movement. *B*, plot of $i_{Na,max}$ against absolute value of membrane potential for currents in *A*. Arrow indicates V_{Na} = 54 mV.

The action potential obtained when the pulse applied under current-clamp conditions exceeds the threshold value (around −65 mV from a holding potential of −90 mV) is illustrated in Fig. 2*B*. The response of the membrane to a subthreshold pulse and three suprathreshold pulses of increasing strength is shown. This is a typical example of the action potentials recorded here in K^+-free external Ringer solution.

Measurement of ionic currents

Good voltage-clamp control of the membrane could be attained with an A-gap of not more than 100 μm and maximum amplifier gain. Under these conditions the

currents were smoothly graded, with no evidence for the second inward component reported by other authors (Hille & Campbell, 1976; Mandrino, 1977).

Fig. 3*A* shows a series of early currents recorded after blocking K^+ currents with tetraethylammonium (TEA) and Cs^+. The transients during depolarizing test pulses were summed with those in response to a constant 50 mV hyperpolarizing control

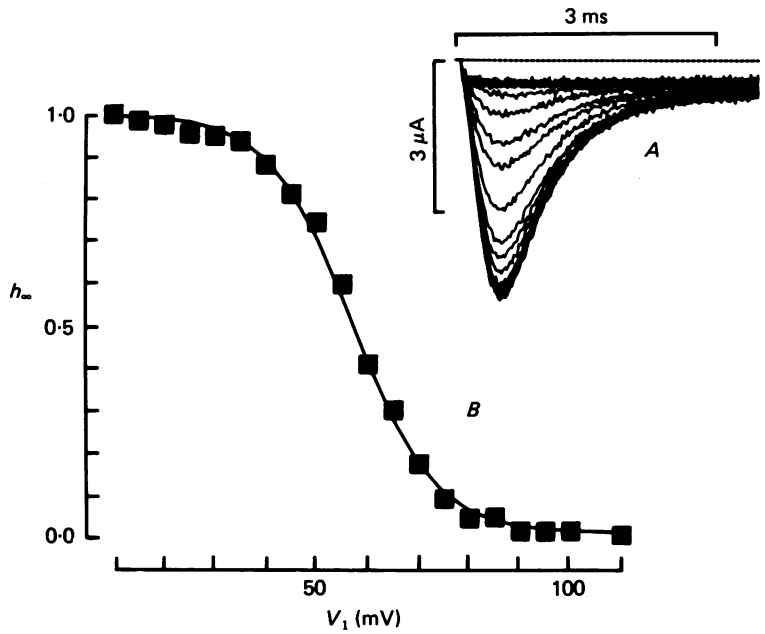

Fig. 4. Steady-state inactivation. External solution A 1 at 14 °C. Cut ends in solution E and C. Surface membrane area in pool A = $2{\cdot}77 \times 10^{-4}$ cm². *A*, superimposed records of Na^+ current for a test pulse, V_2, to −5 mV, following a 20 ms depolarizing pre-pulse, V_1, increasing in 5 mV steps from the holding potential, −105 mV. Decreasing peak current corresponding to increasing depolarizing pre-pulse. Pedestal of rectifying leakage current remains when Na^+ current completely inactivated. *B*, h_∞ curve plotted as

$$\frac{[i_{\mathrm{Na,max}}(V_1, V_2)]}{[i_{\mathrm{Na,max}}(V_1 = 0, V_2)]}$$

against the size of the pre-pulse, V_1, corresponding to records in *A*. Parameters from fit of eqn. (2*b*) to the points: $\frac{C}{A} = 0{\cdot}111 \times 10^{-2}$; $D-B = 0{\cdot}118$ mV^{-1}. From

$$\frac{\mathrm{d} \ln h_\infty}{\mathrm{d}V} = -(D-B)(1-h_\infty),$$

33·9 mV for an *e*-fold change in h_∞ at $h_\infty = 0{\cdot}5$, and 8·5 mV for an *e*-fold change as h_∞ approaches zero.

pulse (multiplied by the ratio size of test pulse/size of control pulse). The net currents obtained in this manner decay to a steady level below the zero line, as can be seen clearly in Fig. 3*A*, parts *a* and *b*. This is attributed to an inwardly rectifying component of the leakage current, since it is insensitive to application of 230 nM-TTX. For pulses taking the membrane potential near the reversal potential (part *a*, lower trace) an initial outward transient can be detected (indicated by the arrow), which

is thought to be a contribution from charge movement within the membrane (Armstrong & Bezanilla, 1974). This initial transient forms the subject of the following paper (Collins *et al.* 1982).

Fig. 3*B* shows the current–voltage relation. The absolute value of the reversal potential for the early transient currents, V_{Na} (subscript indicates Na^+ channel rather than Na^+ ions), was taken at the point where the straight line crosses the horizontal axis. The permeability ratio, $\alpha = P_{Cs}/P_{Na}$, was then determined using the Goldman–Hodgkin–Katz potential equation (Goldman, 1943; Hodgkin & Katz, 1949)

$$V_{Na} = \frac{RT}{ZF} \ln \frac{[Na^+]_o}{[Na^+]_i + \alpha[Cs^+]_i}, \quad (1)$$

where the other parameters have their usual meaning. In nine experiments, the average V_{Na} was $44{\cdot}6 \pm 9{\cdot}9$ mV, which gives an average permeability ratio α of $0{\cdot}145 \pm 0{\cdot}072$. Table 1 in Hille & Campbell (1976) gives V_{Na} as 64 ± 2 mV with 120 mM-Cs^+ and no Na^+ in pools C and E. The corresponding α is $0{\cdot}069 \pm 0{\cdot}005$.

TABLE 2. Steady-state parameters from h_∞–V_1 curves

Experiment		V_h (mV)	V_{Na} (mV)	$\frac{C}{A}$	D–B (mV^{-1})	Temp (°C)
800423a	(▼)	−115	40	$0{\cdot}153 \times 10^{-2}$	0·139	14·8
800423b	—	−110	30	—	—	14·8
800423c	(▲)	−110	57	$0{\cdot}641 \times 10^{-2}$	0·152	14·8
800424a	(■)	−105	55	$0{\cdot}111 \times 10^{-2}$	0·118	14·0
800424b	—	−105	35	—	—	14·0
800513a	(●)	−100	50	$0{\cdot}460 \times 10^{-2}$	0·103	16·6
800513b	—	−100	50	—	—	16·6
800513c	—	−100	50	$0{\cdot}397 \times 10^{-2}$	0·105	16·1
800625	(◪)	−90	34	—	—	18·0
Average		—	44·6	$0{\cdot}35 \times 10^{-2}$	0·12	
±S.D.		—	9·9	$0{\cdot}22 \times 10^{-2}$	0·02	

$\frac{C}{A}$, $D-B$ from fit of equation, $h_\infty = 1{\cdot}0 \Big/ \left(1 + \frac{C}{A} \exp(D-B) \Big/ V_1\right)$ to the points.
Symbols refer to points in Figs 8 and 10.

The true value of the holding potential was determined from the position on the h_∞–V_1 curve, where V_1 is the pulse size for a 20 ms pulse directly preceding the test pulse. The effect of increasing depolarization during V_1 on the Na^+ current flowing in response to a test pulse of constant size is shown in the inset to Fig. 4.

The criteria for determining V_h were that the resting potential in these fibres is −90 mV and that 90 % of the Na^+ channels are available for activation in the resting state (Adrian, Chandler & Hodgkin, 1969). h_∞ is described as

$$h_\infty = \frac{\alpha_h}{\alpha_h + \beta_h}. \quad (2a)$$

Experimental points for h_∞–V_1 were fitted using the equation

$$h_\infty = \frac{1}{1 + \frac{C}{A} \exp(D-B)\, V_1}, \quad (2b)$$

and the derived parameters $\frac{C}{A}$, $D-B$, from five fibres are given in Table 2. The parameters are related to the effective valence (a) of the inactivation gate as follows

$$D-B=\frac{-a}{kT}, \tag{3}$$

$$\ln\frac{C}{A}=\frac{aV'}{kT}, \tag{4}$$

where V' is the transition potential and $kT = 24{\cdot}4$ meV (Rojas, 1975). From the average values in Table 2, $a = 2{\cdot}93\ e$, $V' = -47$ mV.

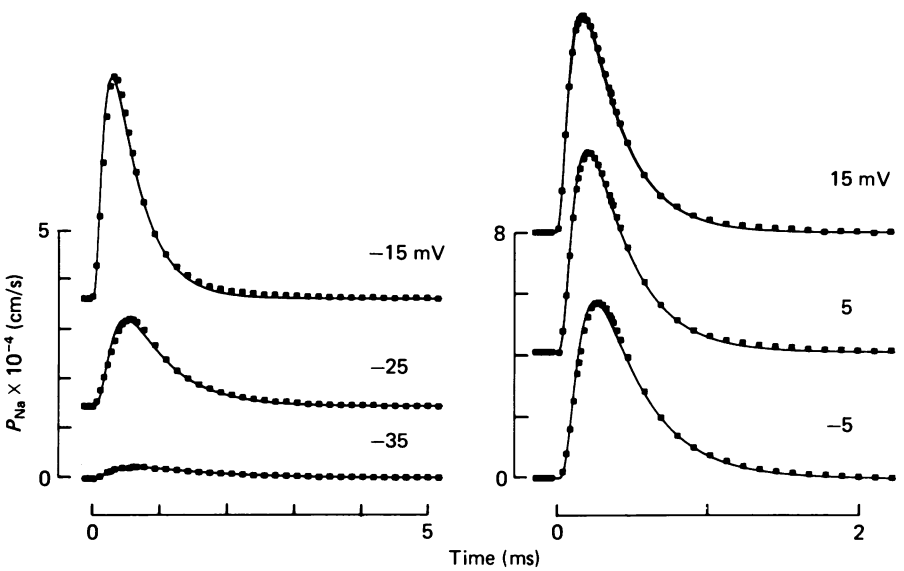

Fig. 5. Time course of $P_{Na}(t)$. Cut ends of fibre in solution E and C. $V_h = -105$ mV. Surface membrane area pool $A = 2{\cdot}60 \times 10^{-4}$ cm^2. Temperature = 17 °C. Points represent subtraction of transient obtained in solution A 4 from transient obtained in solution A 1 for each value of the membrane potential (indicated above each record). Fitted curves are least-squares fits of eqn. (5a)–(5d) to the points. Curves are uncorrected for the effect of a 30 kHz filter in front of the analogue-to-digital converter. Time constants in μs (in order of depolarizing membrane potential): $\tau_m = 220, 203, 129, 103, 86, 74$; $\tau_h = 1297, 630, 409, 314, 272, 249$.

The voltage dependence of the kinetic parameters for activation of the Na^+ current will depend on the model chosen to describe the channel kinetics. The instantaneous current–voltage curve measured in skeletal muscle fibres demonstrates a non-linearity which suggests that the channel kinetics may be better described by the Goldman–Hodgkin–Katz permeability equation than by the conductance equation (Campbell & Hille, 1976). Thus

$$P_{Na} = \bar{P}_{Na}\, m^3 h, \tag{5a}$$

where

$$P_{Na} = i_{Na}\frac{RT}{F^2 V_p}\frac{1}{[Na]_o}\frac{e^{V_p F/RT}-1}{e^{(V_p-V_{Na})F/RT}-1} \tag{5b}$$

V_p is the value of the membrane potential during the pulse.

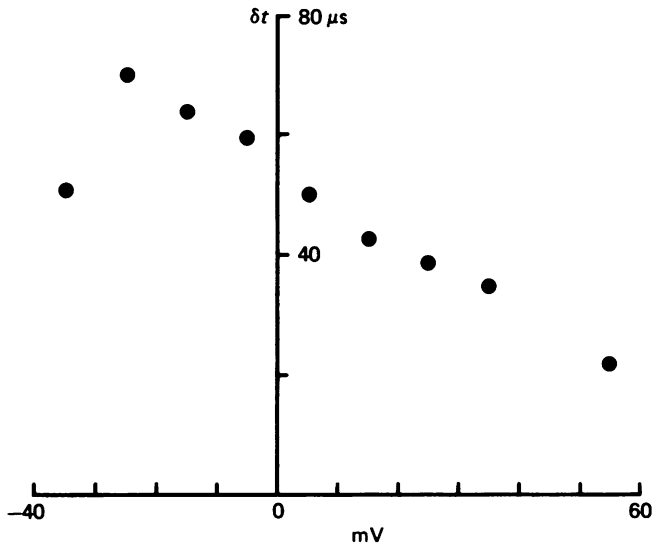

Fig. 6. Voltage dependence of δt. δt from fit of eqn. (5a)–(5d) to $P_{Na}(t)$ in Fig. 5.

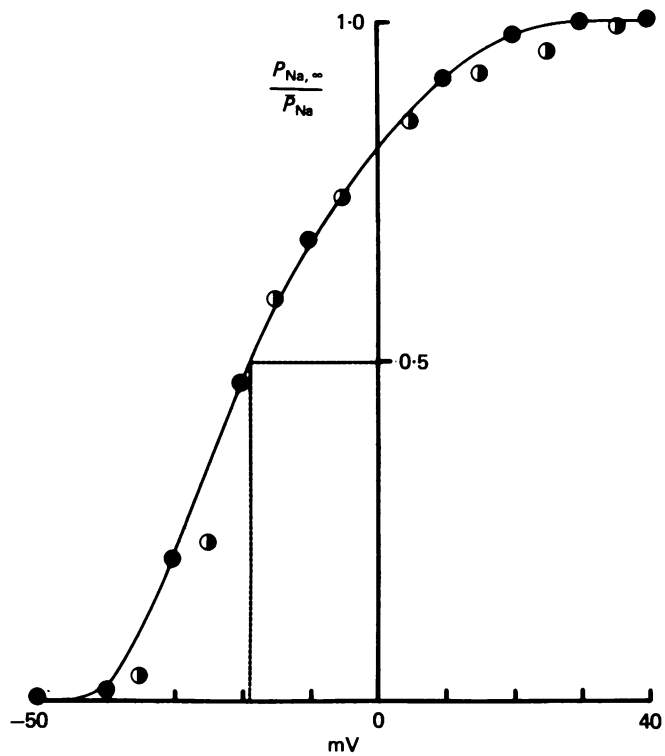

Fig. 7. Voltage-dependence of $P_{Na,\infty}/\bar{P}_{Na}$. ●, P_{Na} measured with single control amplifier voltage clamp. Pool A perfused with solution A 1 at 16·1 °C. Holding potential = −100 mV. Surface membrane area in pool A = $5{\cdot}43 \times 10^{-4}$ cm^2. $\bar{P}_{Na} = 6{\cdot}2 \times 10^{-4}$ cm s^{-1}. Curve drawn through points by eye. ◐, voltage clamp in double control amplifier configuration. Same fibre as Fig. 5. $\bar{P}_{Na} = 7{\cdot}5 \times 10^{-4}$ cm s^{-1}.

Fig. 5 shows a series of $P_{Na}(t)$ curves for inward Na^+ currents in the membrane potential range -35 to 15 mV. Correction for linear capacity and leakage currents was obtained by subtracting from the total current for a depolarizing pulse, the current obtained with the same pulse size, but in the presence of 230 nM-TTX. The TTX-sensitive component was then fitted with eqn. (5*a*) following the procedure of Keynes & Rojas (1976) where

$$m(t) = m_\infty - (m_\infty - m_0)\, e^{-(\delta t + t)/\tau_m} \quad (5c)$$

$$h(t) = h_\infty - (h_\infty - h_0)\, e^{-t/\tau_h} \quad (5d)$$

assuming that h_∞ is 1 and m_0 is 0 at the holding potential of -100 mV.

The voltage dependence of the delay to activation, δt, using eqns (5*a*)–(5*d*) is shown in Fig. 6.

TABLE 3. Change in parameters with fitting procedure

$h_0 = A$ (μA)		$\tau_h = 1/B$ (μs)		$\tau_m = 1/D$ (μs)		$\delta t = (\ln C)/D$ (μs)	
A	B	A	B	A	B	A	B
2·13	2·21	1·41	1·41	367	367	104	108
5·24	5·24	0·91	0·91	244	244	87	72
6·81	6·92	0·67	0·67	179	179	74	59
7·20	7·04	0·55	0·55	130	130	70	46
Aver. % change	2·04		0		0		18·7

A: fitting procedure according to Keynes & Rojas, 1976.
B: fitted with four free parameters in the form $(1 - Ce^{-Dt})^3 Ae^{-Bt}$ as described in the text.

The values for $P_{Na,\,max}$ after correction for inactivation, $P_{Na,\,\infty}$, normalized to the maximum permeability, P_{Na}, have been plotted as a function of membrane potential in Fig. 7 for data acquired with both voltage-clamp configurations.

The function saturates at an absolute membrane potential of 30 mV, with average $\bar{P}_{Na}$ equal to 7×10^{-4} cm s^{-1} and, for an external solution containing 1·8 mM-Ca^{2+} at pH = 7·2, the mid-point potential was -19 mV.

Several $P_{Na}(t)$ records were selected at random and subjected to a fitting procedure which minimizes the sums of squares of the residuals (experimental points − theoretical points) with four free parameters (h_0, τ_h, m_0, τ_m) and a fixed exponent, 3. The values of the parameters obtained from the previous fitting procedure were used to initialize the subroutine, and it was found that h_0, τ_h and τ_m did not change significantly from the first estimate (see Table 3). δt calculated as $\tau_m \ln m_0$, changed by an average of 18·7 %.

The kinetic and steady-state parameters for activation from four fibres are given in Table 4. m_∞ was calculated as $(P_{Na,\,\infty}/\bar{P}_{Na})^{\frac{1}{3}}$. The rate constants α_m and β_m were calculated according to the equations given in the legend to Fig. 8, after normalizing τ_m to 15 °C using $Q_{10} = 2$ (Frankenhaeuser, 1960).

In Fig. 8 the activation parameters have been plotted as a function of voltage. The fitted curve in Fig. 8*D* represents a least-squares fit of a single exponential of the form $a \exp(-bV)$ to β_m–V_p. α_m–V_p (Fig. 8*C*) was found to be linear in the range -30

to 30 mV and could be well fitted with a linear exponential (Tsien & Noble, 1969) of the form $(A+BV)/(1-\exp C(A+BV)/B)$. The parameters of the fit are given in the Figure legend. These were used to reconstruct a fit to the $\tau_m - V_p$ and $m_\infty - V_p$ curves illustrated in Fig. 8*A* and *B*. A value for $\tau_{m,max}$ of 430 μs occurred at −43 mV. The sigmoid curve for m_∞ decays to zero at around −70 mV, dm_∞/dV_p at the mid-point being 0·032 mV^{-1}.

TABLE 4. Kinetic and steady-state parameters for activation

Experiment	V_p (mV)	τ_m (μs)	m_∞	α_m (ms^{-1})	β_m (ms^{-1})	Temp. (°C)
800513a (●)	−50	131	0·15	0·993	5·629	16·6
	−40	332	0·27	0·707	1·911	
	−30	388	0·61	1·368	0·874	
	−20	217	0·80	3·200	0·800	
	−10	179	0·90	4·369	0·485	
	0	144	—	—	—	
	10	127	1·00	6·819	0·000	
	20	96	0·97	8·818	0·273	
	30	79	0·99	10·879	0·110	
800513b (◑)	−40	449	0·32	0·648	1·377	16·6
	−30	390	0·64	1·492	0·839	
	−20	249	0·9	3·285	0·365	
	−10	181	0·95	4·774	0·251	
	0	149	—	—	—	
	10	119	0·97	7·405	0·229	
	20	95	0·96	9·143	0·381	
	30	95	1·00	9·524	0·000	
800424a (■)	−40	367	0·27	0·818	2·212	14·0
	−30	283	0·56	2·116	1·725	
	−20	209	0·77	4·015	1·223	
	−10	172	0·93	5·569	0·419	
	0	151	1·99	7·279	0·074	
	10	112	1·00	8·264	0·000	
800625 (◪)	−40	491	0·26	0·400	1·168	18·0
	−30	315	0·53	1·290	1·149	
	−20	209	0·83	3·044	0·632	
	−10	142	0·90	4·870	0·535	
	0	85	—	—	—	
	10	82	0·98	9·121	0·224	
	20	67	1·00	11·494	0·000	

τ_m uncorrected for temperature.
α_m, β_m calculated using τ_m normalized to 15 °C assuming $Q_{10} = 2·0$.

The kinetic parameters for inactivation in the range −50 to 30 mV were obtained from the fit to $P_{Na}(t)$ but, in order to extend the voltage axis into the negative region, a double-pulse protocol was employed (Hodgkin & Huxley, 1952*a*). The membrane was stepped up to a depolarized level and a test pulse applied at increasing intervals (T = 0·1–25 ms) from the onset of the step. The dependence of $i_{Na,max}$ for the test pulse, on interval time, was plotted for each voltage level (Fig. 9). The fitted curves are a least-squares fit of a single exponential to the points and the time constant is assumed to be τ_h.

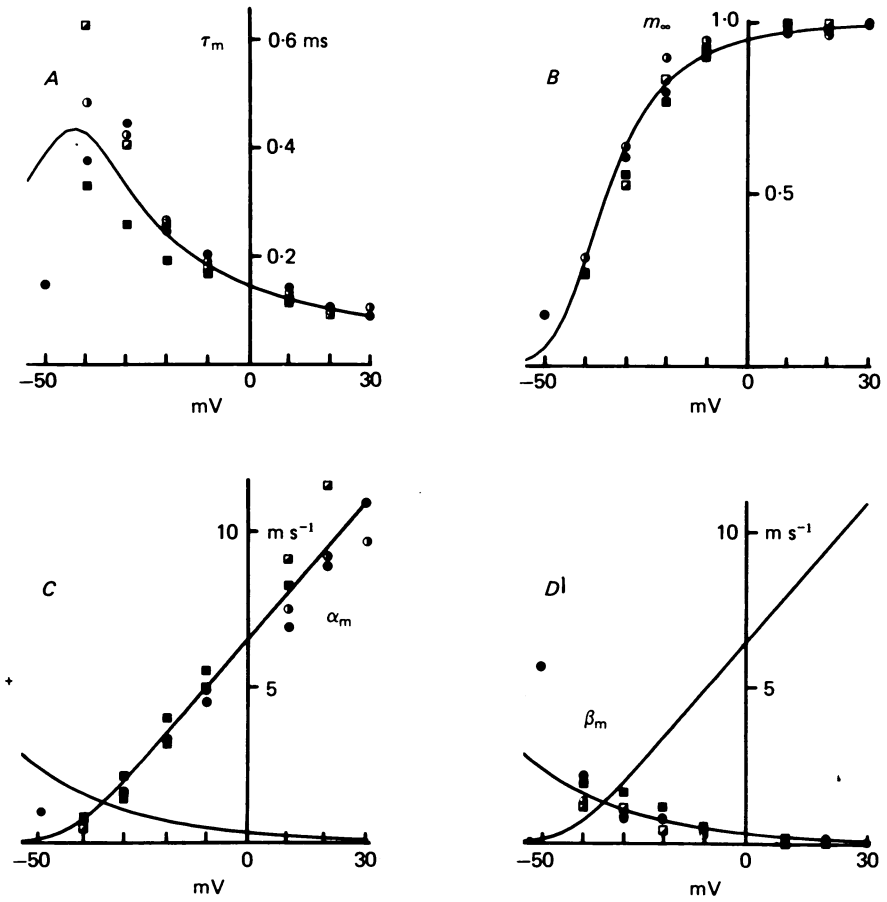

Fig. 8. Kinetic and steady-state parameters for activation. *A*, τ_m, points normalized to 15 °C using $Q_{10} = 2$. Curve fitted using $\tau_m = 1/(\alpha_m + \beta_m)$. *B*, m_∞, curve fitted using $m_\infty = \alpha_m/(\alpha_m + \beta_m)$. *C*, α_m, points calculated using $\alpha_m = m_\infty/\tau_m$. Curve fitted using $\alpha_m = (A + BV)/(1 - \exp(C(A + BV)/B)$, where $A = 6{\cdot}39$, $B = 0{\cdot}15$ mV^{-1}, $C = -0{\cdot}3$. β_m curve added for comparison. *D*, β_m, points calculated using $\beta_m = (1 - m_\infty)/t_m$. Curve fitted using $\beta_m = a \exp bV$ where $a = 0{\cdot}33$, $b = -0{\cdot}04$ mV^{-1}. α_m curve added for comparison. Symbols refer to experiments as in Table 2.

Fig. 10 shows the voltage dependence of the kinetic parameters for inactivation, fitted in a similar manner to the activation parameters. τ_h was normalized using $Q_{10} = 3$ (Frankenhaeuser, 1960) and gave a maximum of 925 μs at −78 mV. The mid-point potential of the h_∞ curve occurred at −73 mV and $h_\infty = 1$ at −103 mV. α_h could be well fitted with a single exponential, whereas β_h was better described by a linear exponential function as for α_m. The parameters of the fit are given in the legend to Fig. 10.

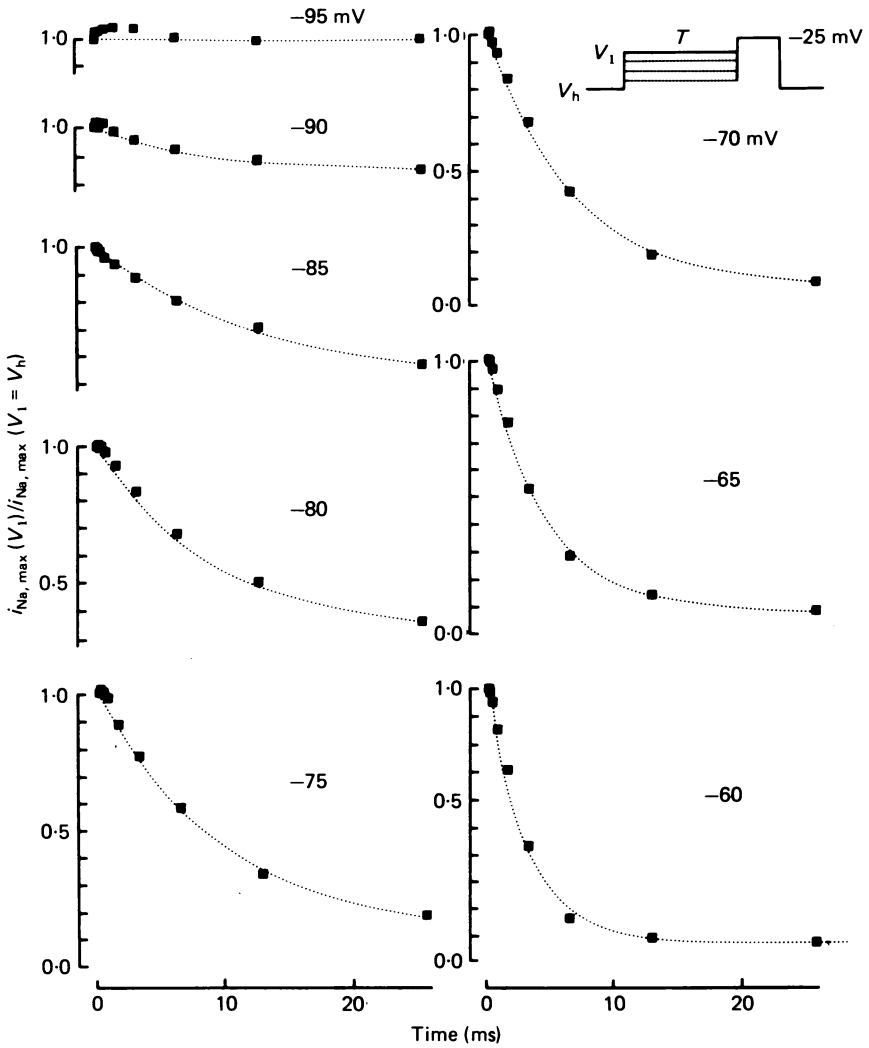

Fig. 9. Time course of onset of inactivation for negative membrane potentials. Pool A perfused with solution A 2 at 14·8 °C. Holding potential (V_h) set at −115 mV. Surface membrane area in pool A = $4·09 \times 10^{-4}$ cm². Horizontal axis, pre-pulse duration (T) in ms. Numbers above each record indicate absolute value of membrane potential during the pre-pulse (V_l). Points represent $i_{Na,max}$ for increasing pre-pulse duration normalized to $i_{Na,max}$ for the test pulse without pre-pulse. Fitted curves represent fit of a single exponential to the points. Insert shows the pulse protocol.

Slow inactivation of the Na^+ current

The double-pulse procedure used to induce a slow inactivation of the Na^+ current is illustrated at the top of Fig. 12. While the pre-pulse duration (T) was varied from 0 to 3 s, the period of repolarization at the holding potential (−120 mV) before the test pulse was kept constant at 0·05 s. At −120 mV h_∞ is close to 1, signifying that

a maximum number of Na^+ channels are available for activation. The absolute membrane potential during the pre-pulse was 30 mV to allow a direct comparison with results from the charge displacement in these fibres presented in the following paper. A single test voltage was used in these experiments since individual runs are necessarily long events. All measurements were made in the linear region of the I–V curve, in which effects due to lack of voltage-clamp control over the whole membrane area are minimal.

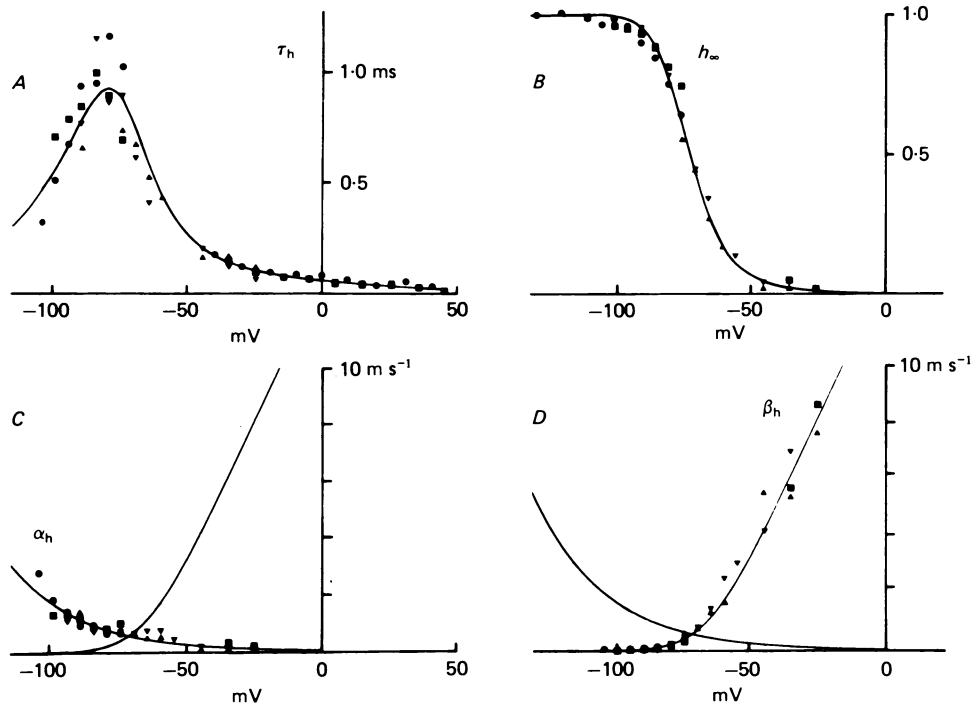

Fig. 10. Kinetic and steady-state parameters for activation. A, τ_h, points normalized to 15 °C assuming $Q_{10} = 3$. Curve fitted using $\tau_h = 1/(\alpha_h+\beta_h)$. B, h_∞, curve fitted using $h_\infty = \alpha_h/(\alpha_h+\beta_h)$. C, α_h, points calculated using $\alpha_h = h_\infty/\tau_h$. Curve fitted using $\alpha_h = A\exp BV$, where $A = 0{\cdot}04$, $B = -0{\cdot}038$ mV^{-1}. β_h curve added for comparison. D, β_h, points calculated using $\beta_h = (1-h_\infty)/\tau_h$. Curve fitted using $\beta_h = (a+bV)/(1-\exp(c(a+bV)/b)$ where $a = 13{\cdot}24$, $b = 0{\cdot}2$ mV^{-1}, $c = -0{\cdot}18$. α_h curve added for comparison. Symbols refer to experiments as in Table 2.

The recovery from slow inactivation was measured by holding the membrane at an absolute potential of 30 mV for 3 s and varying the duration of the repolarization interval from 0·02 to 3 s.

In Fig. 11 the Na^+ current for an absolute membrane potential of −10 mV is shown for a series of pre-pulse durations (traces corresponding to A). The fit of a single exponential function to the inactivation phase is shown, and the result of dividing the fitted exponential into the array containing the experimental points is the Na^+ current corrected for fast inactivation (traces corresponding to B). The steady level is then $i_{Na,\infty}$.

Fig. 12*A* and *B* shows the time course for development of ('on') and recovery from ('off') slow inactivation. Normalized values for both $i_{Na,max}$ (●) and $i_{Na,\infty}$ (◑) are plotted, and are seen to vary in a similar manner with T. This indicates that the underlying relation between τ_m and τ_h remains unchanged during slow inactivation. The kinetic parameters from the fit of $\bar{\imath}_{Na}m^3h$ to $i_{Na}(t)$ are given in Table 5. τ_h, τ_m and δt do not appear to be modulated by the length of the conditioning pre-pulse.

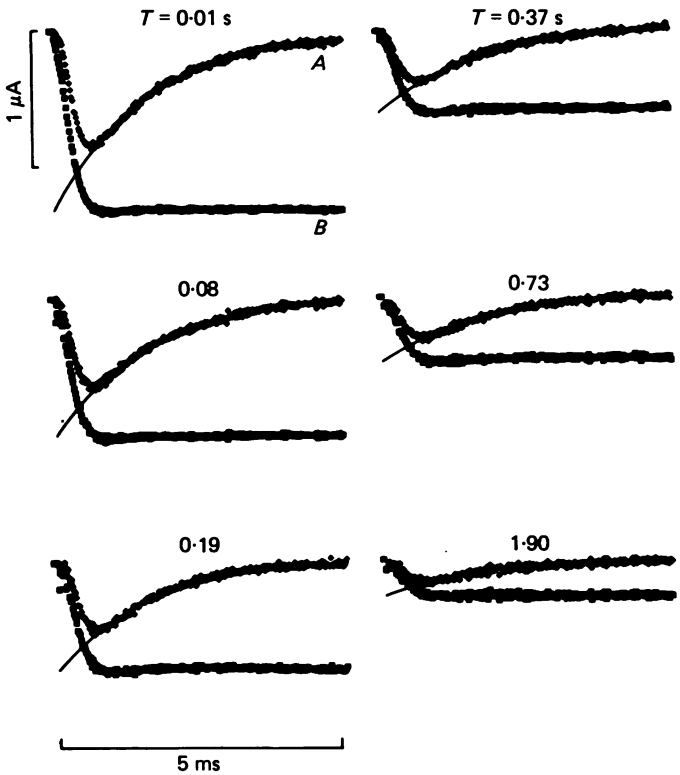

Fig. 11. Na^+ currents with increasing pre-pulse duration. External solution A 1 at 10·5 °C. Cut ends in contact with solution E and C. $V_h = -100$ mV. Inward Na^+ currents (labelled *A* in top left segment) in response to $V_p = -10$ mV, with increasing pre-pulse duration, T, given in seconds above each record. Continuous line represents a single exponential least-squares fit to the points during the inactivation phase. Time constant, $\tau_h = 1{\cdot}18$ ms. Traces corresponding to *B* are Na^+ current corrected for fast inactivation. Steady level is $i_{Na,\infty}$.

At 13 °C, 95 % of the Na^+ channels were inactivated after 3 s. In Fig. 12*C* the values for $i_{Na,max}$ have been reduced according to the equations shown in the inset, and plotted semilogarithmically against T. The 'on' values fall on a straight line, indicating a single time constant for the development of slow inactivation, $\tau = 0{\cdot}58$ s. For values of T smaller than 1 s, the 'off' values fall on the same line.

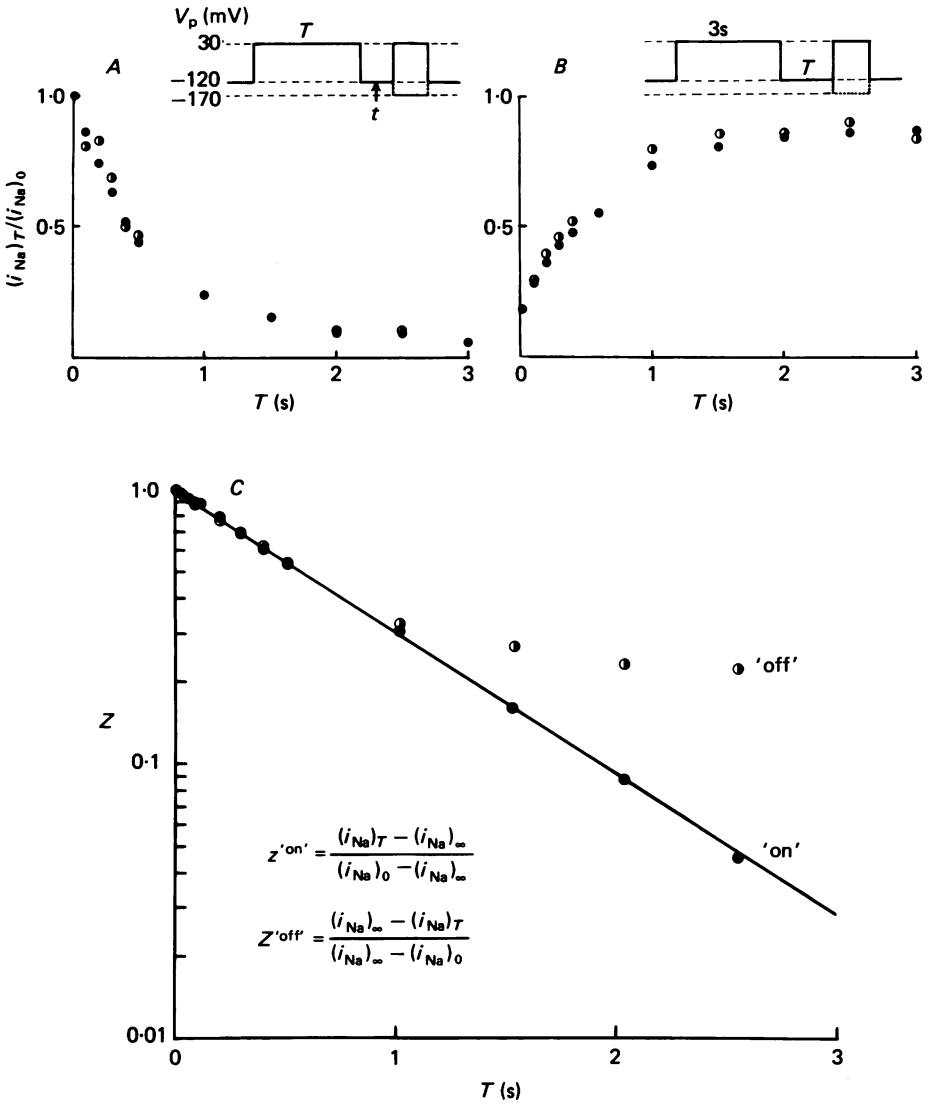

Fig. 12. Time course of slow inactivation. External solution A 1 at 13 °C. Cut ends in contact with solution E and C. Holding potential set at −120 mV. Surface membrane area in pool A = $2{\cdot}07 \times 10^{-4}$ cm².

Upper part, symbols represent:

$$◑ = \frac{(i_{Na,\infty})_T}{(i_{Na,\infty})_0}, \quad ● = \frac{(i_{Na,max})_T}{(i_{Na,max})_0}$$

A, development of slow inactivation ('on') with increasing pre-pulse duration (T), constant gap width (t = 0·05 s) and test pulse to V_p = 0 mV. *B*, recovery from slow inactivation ('off') with increasing gap width (T), constant pre-pulse (3 s) and test pulse to 0 mV. *C*, *reduced* values for $i_{Na,max}$ (Z calculated according to the equations shown in the inset) plotted semilogarithmically against T. Straight line is the linear regression to the points for 'on'. Time constant = 0·58 s with r^2 = 0·99. Pulse protocols shown above *A* and *B*.

DISCUSSION

Measurements of $i_{Na,max}$ were made in this work with 50% of the Na^+ channels blocked by external application of TTX. The full Na^+ current should, therefore, be twice as large. However, since absolute values for membrane current, as referred to area of surface membrane, depend heavily on the method used to calculate the calibration factor for the measured voltage (gain $\times R_{ED} \times$ area)$^{-1}$, the area estimated

TABLE 5. Parameters from fit to Na^+ currents; development of slow inactivation

Pre-pulse (s)	$i_{Na,max}$ (μA)	$i_{Na,\infty}$ (μA)	τ_m (μs)	τ_h (μs)	δt (μs)
0·00	2·39	6·71	207	781	80
0·02	2·26	6·34	184	756	93
0·04	2·07	5·79	186	766	88
0·06	1·88	5·40	205	754	77
0·08	1·71	5·04	211	731	84
0·09	1·56	4·67	216	762	80
0·00	1·57	4·57	199	758	81
0·10	1·35	3·71	191	793	83
0·21	1·16	3·80	221	700	81
0·31	0·99	3·14	223	742	75
0·41	0·81	2·30	207	794	82
0·51	0·70	2·14	227	763	77
0·00	1·20	3·15	188	828	77
0·51	0·61	1·72	201	801	81
1·02	0·29	0·76	230	795	86
1·54	0·19	0·51	207	865	65
2·05	0·12	0·36	228	769	73
2·56	0·11	0·32	240	794	74
3·07	0·07	0·18	193	799	61

from geometrical measurements represents a possible source of error, which increases as geometry is decreased. As previously suggested, the membrane area measured here is probably underestimated by a factor close to 2, and thus the values for i_{Na} and P_{Na} quoted per surface membrane area may be considered equivalent to those for a membrane with 100% unblocked Na^+ channels.

In Table 6 some of the kinetic parameters from previous analyses of the Na^+ channel in skeletal muscle using the Hodgkin–Huxley model have been collated. The time constants have been adjusted to 15 °C for comparative purposes (numbers in parentheses), using a Q_{10} of 2 for τ_m and a Q_{10} of 3 for τ_h as in this analysis. $\tau_{m,max}$ ranges between 329 and 430 μs, $\tau_{h,max}$ between 0·9 and 7·2 ms.

The position of the h_∞–V_1 curve (given by $V_{h\frac{1}{2}}$) varies between −58 and −84 mV. For the m_∞–V_p curve, the mid-point potential varies between −35 and −50 mV. This variation may be a consequence of holding potential since both values are more negative for the more positive holding potential of −90 mV as compared to −100 mV.

The temperature effect of Na^+ conductance has been described for nerve membranes (Moore, 1971) as a change equivalent to 4% per °C. The conductance values given

TABLE 6. Comparison of results with previous work

Authors	Voltage clamp	Temp. (°C)	V_h (mV)	E_{Na} (mV)	$i_{Na,max}$ (mA/cm²)	$\bar{g}_{leak}$ (mS/cm²)	$V_{h\frac{1}{2}}$ (mV)	$V_{m\frac{1}{2}}$ (mV)	$\tau_{h,max}$ (ms)	$\tau_{m,max}$ (μs)	$\bar{g}_{Na}$ (mS/cm²)
Adrian *et al.* (1970)	3-micro-electrode	1–3	−100	20	0·5	0·5–1·0	−65	−40	30 (7·2) (at −47 mV)	—	70 (106)
Ildefonse & Rougier (1971)	Double sucrose gap	20–24	−90	38*	1·06*	—	−79	−50	3 (6·5) (at −75 mV)	200 (329) (at −50 mV)	—
Campbell & Hille (1976)	Vaseline gap	5	−90	64	3·7	—	−79	−44	12 (4) (at −75 mV)	300 (150) (at −40 mV)	73 (102)†
This work	Vaseline gap	15	−100	43	6–13	0·95	−58	−35	0·9 (at −78 mV)	430 (at −43 mV)	214

Resting potential taken as −90 mV except in work of Adrian *et al.* (1970), −95 mV.
$V_{h\frac{1}{2}}$, mid point of h_∞ curve. $V_{m\frac{1}{2}}$, mid point of m_∞ curve.
* Value given by Ildefonse & Roy (1972).
Time constant in parentheses adjusted using a Q_{10} of 2 for τ_m and Q_{10} of 3 for τ_h.
$\bar{g}_{Na}$ in parentheses adjusted assuming a change of 4 % per °C.
† Maximum chord conductance.

in parentheses in Table 6 have been normalized to 15 °C according to this coefficient. However, since Campbell & Hille (1976) quote maximum chord conductance rather than $\bar{g}_{Na}$, their value must be multiplied by 2 to give a minimum correction for inactivation. The resulting 204 mS/cm² is then comparable to the value obtained here, namely 214 mS/cm².

Since the tubular membrane system contributes such a large part of the total capacity of the muscle fibre (approximately three times that of the surface membrane, giving a total capacity of 3–6 μF/cm² referred to area of surface membrane (see Collins *et al.* 1982), it has been suggested that activity in the T-system could be contributing to the ionic current detected in pool A (Hille & Campbell, 1976; Mandrino, 1977). A slow component, attributed to diffusion time for the TTX molecule through the T-system has been detected in the TTX binding kinetics of muscle membranes (Allen *et al.* 1980), in which it is implicit that a portion of the recorded ionic current has its origin in the T-system.

Since the current records here did not exhibit 'secondary bumps' (Mandrino, 1977) the amplitude of the hypothetical tubular current cannot be estimated. From the Disk equivalent circuit (Adrian & Peachey, 1973) Hille & Campbell (1976) estimated $\bar{P}_{Na}$ for the tubular membrane as 1·3% that for the surface membrane at −30 mV and 5 °C. If we assume that the permeability of surface and tubular membranes have the same Q_{10}, we could estimate a $\bar{P}_{Na}$ of 2×10^{-6} cm s^{-1} for the tubular membrane at 15 °C, on this basis. It is of course unlikely that the tubular membrane will be under voltage-clamp control.

An implicit assumption in the analysis of currents through the Na^+ channel on the Hodgkin–Huxley model is that the inactivation is controlled specifically by the h variable. However, this model does not describe the effects of long depolarizations on the permeability system, when it has been found necessary to introduce an extra variable with a much larger time constant than τ_h. A slow inactivation of the Na^+ current has been described for the lobster giant axon (Narahashi, 1964), squid giant axon (Adelman & Palti, 1969), *Myxicola* giant axon (Schauf, Pencek & Davis, 1976) and *Xenopus* myelinated nerve fibres (Brismar, 1978), with time constants in the range 0·3–10 s; also an 'ultra-slow' Na^+ inactivation has been described for frog myelinated nerve fibres (Neumcke, Fox, Drouin & Schwarz, 1976), with time constant 2–4 min. The time constant for frog muscle measured here (0·58 s) falls within the range of values for slow inactivation in other preparations. Although the mechanism for slow inactivation remains unresolved, the development of the effect in these muscle fibres in a K^+-free media indicates that external K^+ is not a requirement. This result is different from that obtained for the node of Ranvier (Peganov, Khodorov & Shiskova, 1973).

At first glance, it seems that there are large variations in the kinetic parameters of the ionic current as determined by different experimental techniques. Where the behaviour of the variable is known (e.g. temperature), a correction factor may be introduced which narrows the range of values. The data presented in this work become comparable, especially to the previous data on the same muscle preparation, using the same voltage-clamp system. However, in the light of the differences exhibited, the necessity for a complete analysis of the Na^+ currents to provide a true comparison with the properties of the fast charge movements in the same system must be recognized.

We would like to thank Dr P. Pynsent for setting up the computer system, Professor Nelson Arispe and Miss E. Quinta-Ferreira for helpful advice and criticism, and Mrs S. Garrod for secretarial assistance. This work formed part of a thesis by C.A.C. for the degree of Ph.D. at the University of East Anglia. The research was financially supported by the Science Research Council.

REFERENCES

ADELMAN, W. R. & PALTI, Y. (1969). The effects of external potassium and long duration voltage conditioning on the amplitude of sodium currents in the giant axon of the squid *Loligo pealei*. *J. gen. Physiol.* **54**, 589–606.

ADRIAN, R. H., CHANDLER, W. K. & HODGKIN, A. L. (1970). Voltage clamp experiments in striated muscle fibres. *J. Physiol.* **208**, 607–644.

ADRIAN, R. H. & PEACHEY, L. D. (1973). Reconstruction of the action potential of frog sartorius muscle. *J. Physiol.* **235**, 103–131.

ALLEN, T. J. A., ROJAS, E. & SUAREZ-ISLA, B. (1980). The rate of action of tetrodotoxin on sodium conductance in frog skeletal muscle fibres. *J. Physiol.* **308**, 100–101*P*.

ARMSTRONG, C. M. & BEZANILLA, F. (1974). Charge movement associated with the opening and closing of the activation gates of the Na^+ channel. *J. gen. Physiol.* **63**, 533–552.

BRISMAR, T. (1978). Slow mechanism for sodium permeability inactivation in myelinated nerve fibres of *Xenopus laevis*. *J. Physiol.* **270**, 283–297.

CAMPBELL, D. T. & HILLE, B. (1976). Kinetic and pharmacological properties of the sodium channel of frog skeletal muscle. *J. gen. Physiol.* **67**, 309–323.

COLLINS, CAROL A., ROJAS, E. & SUAREZ-ISLA, B. A. (1982). Fast charge movements in skeletal muscle fibres from *Rana temporaria*. *J. Physiol.* **324**, 319–345.

DODGE, F. A. & FRANKENHAEUSER, B. (1958). Membrane currents in isolated frog nerve fibres under voltage clamp conditions. *J. Physiol.* **143**, 76–90.

FRANKENHAEUSER, B. (1960). Quantitative description of sodium currents in myelinated nerve fibres of *Xenopus laevis*. *J. Physiol.* **151**, 491–501.

GOLDMAN, D. E. (1943). Potential, impedance and rectification in membranes. *J. gen. Physiol.* **27**, 37–60.

HILLE, B. & CAMPBELL, D. (1976). An improved vaseline gap voltage clamp for skeletal muscle fibres. *J. gen. Physiol.* **67**, 265–293.

HODGKIN, A. L. & HUXLEY, A. F. (1952*a*). The dual effect of membrane potential on sodium conductance in the giant axon of *Loligo*. *J. Physiol.* **116**, 497–506.

HODGKIN, A. L. & HUXLEY, A. F. (1952*b*). A quantitative description of membrane current and its application to conduction and excitation in nerve. *J. Physiol.* **117**, 500–544.

HODGKIN, A. L. & KATZ, B. (1949). The effect of sodium ions on the electrical activity of the giant axon of the squid. *J. Physiol.* **108**, 37–77.

ILDEFONSE, M. & ROUGIER, O. (1972). Voltage clamp analysis of the early current in frog skeletal muscle fibre using the double sucrose-gap method. *J. Physiol.* **222**, 373–395.

ILDEFONSE, M. & ROY, G. (1972). Kinetic properties of the sodium current in striated muscle fibres on the basis of the Hodgkin–Huxley theory. *J. Physiol.* **227**, 419–431.

KEYNES, R. D. & ROJAS, E. (1976). The temporal and steady-state relationships between activation of the sodium conductance and movement of the gating particles in the squid giant axon. *J. Physiol.* **255**, 157–189.

KEYNES, R. D., ROJAS, E., TAYLOR, R. E. & VERGARA, J. (1973). Calcium and potassium systems of a giant barnacle muscle fibre under membrane potential control. *J. Physiol.* **229**, 409–455.

MANDRINO, M. (1977). Voltage-clamp experiments on frog single skeletal muscle fibres: evidence for a tubular sodium current. *J. Physiol.* **269**, 605–625.

MOORE, L. E. (1971). Effect of temperature and calcium ions on rate constants of myelinated nerve. *Am. J. Physiol.* **221**, 131–137.

MOORE, J. W. & COLE, K. S. (1963). Voltage clamp techniques. In *Physical Techniques in Biological Research*, vol. VI, Electrophysiological methods, part B., pp. 263–321. ed. NASTUK, W. L. New York and London: Academic Press.

NAKAJIMA, S. & BASTIAN, J. (1974). Double sucrose gap method applied to single muscle fibres of *Xenopus laevis*. *J. gen. Physiol.* **63**, 235–256.

NARAHASHI, T. (1964). Restoration of action potential by anodal polarization in lobster giant axons. *J. cell. comp. Physiol.* **64**, 73–96.

NEUMCKE, B., FOX, J. M., DROUIN, H. & SCHWARZ, W. (1976). Kinetics of the slow variation of peak Na^+ current in the membrane of myelinated nerve following changes of holding potential or extracellular pH. *Biochim. biophys. Acta* **426**, 245–257.

NONNER, W. (1969). A new voltage clamp method for Ranvier nodes. *Pflügers Arch.* **309**, 176–192.

PEGANOV, E. M., KHODOROV, B. I. & SHISKOVA, L. D. (1973). Slow sodium inactivation in the Ranvier node membrane: role of external potassium. *Bull. exp. biol. Med. U.S.S.R.* **76**, 1014–1017.

PYNSENT, P. & ROJAS, E. (1979). Voltage clamp and data acquisition method for single myelinated nerve fibre work. *J. Physiol.* **291**, 14–15*P*.

QUINTA-FERREIRA, E., ARISPE, N. & ROJAS, E. (1982). Sodium currents in the giant axon of the crab *Carcinus maenas*. *J. Membrane Biol.* (In the Press).

ROJAS, E. (1975). Gating mechanism for the activation of the sodium conductance in nerve membranes. *Cold Spring Harb. Symp. quant. Biol.* **40**, 305–320.

SCHAUF, C. L., PENCEK, T. L. & DAVIS, F. A. (1976). Slow sodium inactivation in *Myxicola* axons – evidence for a second inactive state. *Biophys. J.* **16**, 771–778.

TSIEN, R. W. & NOBLE, D. (1969). A transition state theory approach to the kinetics of conductance changes in excitable membranes. *J. Membrane Biol.* **1**, 248–273.

VERGARA, J. & CAHALAN, M. (1978). Charge movements in a skeletal muscle fibre. *Biophys. J.* **21**, 167a.